

# DESIGN, OPTIMIZATION, FORMULATION AND CHARACTERIZATION OF ATORVASTATIN NANOCRYSTALS

**Dr. P Premkumar<sup>1\*</sup>**, Professor, Research Guide, Department of Pharmaceutics, Saveetha College of Pharmacy, Saveetha Institute of Medical and Technical Sciences (SIMATS), Saveetha university, Thandalam, Chennai-602105, India

**Mrs. Jency Abraham<sup>2\*</sup>**, Research Scholar, Saveetha College of Pharmacy, Saveetha Institute of Medical and Technical Sciences (SIMATS), Saveetha university, Thandalam, Chennai-602105, India

**Mrs. Nikhila M Nair,<sup>3</sup>** Research Scholar, Saveetha College of Pharmacy, Saveetha Institute of Medical and Technical Sciences (SIMATS), Saveetha university, Thandalam, Chennai-602105, India

**CORRESPONDENCE AUTHOR: DR. P PREMKUMAR**

DOI: <https://doi.org/10.63001/tbs.2025.v20.i02.S2.pp11-24>

## KEYWORDS

Solubility,  
Bioavailability,  
Nanocrystals,  
Atorvastatin,  
BCS Class 2,  
Lipid lowering agent.

Received on:

12-02-2025

Accepted on:

10-03-2025

Published on:

07-04-2025

## ABSTRACT

The most tedious challenge currently faced by formulation scientists is that of formulation of poorly water-soluble drug moieties. According to literature reports, more than 40% of the drugs being introduced into the formulation research pipeline have poor water solubility. Developments of the drug into nanosized formulations have helped overcome the bioavailability problems of many a poorly water soluble drugs belonging to BCS Class II and IV. One category of such nanosized formulations comprise of nanoscaled drug particles stabilized by a suitable stabilizer or surfactant, referred to as “**Nanocrystals.**”

Attempts were made to improve the solubility of atorvastatin so as to improve its oral bioavailability. A very important issue in nanocrystal formulation is the choice of the stabilizers, which are required to prevent nanoparticle aggregation. Pharmaceutical excipients that can be used as stabilizers include the cellulose, such as hydroxypropyl cellulose (HPC) and hydroxypropylmethyl cellulose (HPMC), povidone (PVP K30), and pluronics (F68 and F127); as well as surfactant stabilizers which can be non-ionic, such as polysorbate (Tween 80), or anionic, such as sodium lauryl sulfate (SLS) and docusate sodium (DOSS).

## INTRODUCTION

Atorvastatin, as a synthetic lipid-lowering agent, is an inhibitor of 3-hydroxy-3-methyl-glutaryl-coenzyme A (HMG-CoA) reductase which catalyses the conversion of HMG-CoA to mevalonate, an early rate-limiting step in cholesterol biosynthesis. It is insoluble in an aqueous solution of pH 4 and below, very slightly soluble in water and slightly soluble at pH 7.4 phosphate buffer, slightly soluble in ethanol and freely soluble in methanol. Atorvastatin is readily permeable at the physiological intestinal pH, yet its oral bioavailability following a 40 mg oral dose does not exceed 12%. Thus, attempts were made to improve the solubility of atorvastatin so as to improve its oral bioavailability. A very important issue in nanocrystal formulation is the choice of the stabilizers, which are required to prevent nanoparticle aggregation. Within this reduced size range, attractive forces between particles appear. These attractive forces arise due to dispersion or van der Waals forces. As particles come close, these attractive forces increase and particle aggregation tends to become irreversible. The added stabilizers act to prevent or

minimize such aggregation through steric or electrostatic stabilization. Steric stabilization is achieved by adsorbing polymers onto the particle surface, whereas electrostatic stabilization is obtained by adsorbing charged molecules, which can be ionic surfactants or charged polymers, onto the particle surface. Pharmaceutical excipients that can be used as stabilizers include the cellulose, such as hydroxypropyl cellulose (HPC) and hydroxypropylmethyl cellulose (HPMC), povidone (PVP K30), and pluronics (F68 and F127); as well as surfactant stabilizers which can be non-ionic, such as polysorbate (Tween 80), or anionic, such as sodium lauryl sulfate (SLS) and docusate sodium (DOSS).

Formulated nanocrystals can be characterized through a number of tests including particle size determination as well as surface charge measurement (zeta potential), particle crystallization and dissolution. In this study, we aim at improving the poor water solubility of atorvastatin calcium, and hence its bioavailability, through size reduction to the nano-size range. The high-pressure homogenization technique has been employed using a variety of stabilizers at various concentrations.

## AIM AND PLAN OF WORK

The most tedious challenge currently faced by formulation scientists is that of formulation of poorly water-soluble drug moieties. Advancement in high throughput screening methods is mainly responsible to an even larger number of newly discovered drugs having poor water solubility. According to literature reports, more than 40% of the drugs being introduced into the formulation research pipeline have poor water solubility. Development of the drug into nanosized formulations have helped overcome the bioavailability problems of many a poorly water soluble drugs belonging to BCS Class II and IV. One category of such nanosized formulations comprise of nano scaled drug particles stabilized by a suitable stabilizer or surfactant, referred to as "Nanocrystals".

Atorvastatin, as a synthetic lipid-lowering agent, is an inhibitor of 3-hydroxy-3-methyl-glutaryl-coenzyme A (HMG-CoA) reductase which catalyzes the conversion of HMG-Co A to mevalonate, an early rate-limiting step in cholesterol biosynthesis. It is insoluble in an aqueous solution of pH 4 and below, very slightly soluble in water and slightly soluble at pH 7.4 phosphate buffer, slightly soluble in ethanol and freely soluble in methanol. Atorvastatin is readily permeable at the physiological intestinal pH, yet its oral bioavailability following a 40 mg oral dose does not exceed 12%. Thus, attempts were made to improve the solubility of atorvastatin so as to improve its oral bioavailability. A very important issue in nanocrystal formulation is the choice of the stabilizers, which are required to prevent nanoparticle aggregation. Within this reduced size range, attractive forces between particles appear. These attractive forces arise due to dispersion or van der Waals forces. As particles come close, these attractive forces increase and particle aggregation tends to become irreversible. The added stabilizers act to prevent or minimize such aggregation through steric or electrostatic stabilization. Steric stabilization is achieved by adsorbing polymers onto the particle surface, whereas electrostatic stabilization is obtained by adsorbing charged molecules, which can be ionic surfactants or charged polymers, onto the particle surface. Pharmaceutical excipients that can be used as stabilizers include the cellulosic, such as hydroxypropyl cellulose (HPC) and hydroxypropyl methyl cellulose (HPMC), povidone (PVP K30), and pluronics (F68 and F127); as well as surfactant stabilizers which can be non-ionic, such as polysorbate (Tween 80), or anionic, such as sodium lauryl sulfate (SLS) and docusate sodium (DOSS). Formulated nanocrystals can be characterized through a number of tests including particle size determination as well as surface charge measurement (zeta potential), particle crystallization and dissolution. In this study, we aim at improving the poor water solubility of atorvastatin calcium, and hence its bioavailability, through size reduction to the nano-size range. The high pressure homogenization technique has been employed using a variety of stabilizers at various concentrations.

## EXPERIMENTAL METHODOLOGY

### Materials

Atorvastatin calcium (ATC) was obtained as a gift sample from Shasun Pharmaceuticals, Pondichery (India). All other chemicals and reagents were of analytical grade purchased from SD fine chemicals, Mumbai. FT-IR spectra were taken using Shimadzu FT-IR-8700 spectrophotometer; DSC thermograms were obtained by differential scanning calorimeter (DSC 60; Shimadzu) where as XRD patterns were recorded using Philips diffractometer (PW3710; Almelo, Netherland).

### Melting Point Determination

Melting point was determined by using glass capillary method. The Thiesle tube filled with paraffin oil was used, in to which a capillary containing the drug was placed along with the thermometer. The paraffin oil was then heated continuously till the powder melts and corresponding temperature was noted and recorded as melting point of drug.

### Standard Calibration Curve of ATC

Standard Calibration Curve of ATC was carried out in Phosphate buffer (pH 6.8)

### Procedure

Accurately weighed 10 mg of ATC was dissolved in required volume of methanol and volume was made up to 100 ml by using Phosphate buffer (pH 6.8) to get 100 µg/ml stock solution. From the above stock, serial dilutions were made by withdrawing 1, 2,

3, 4 and 5 ml solution and diluting up to 10 ml with the same stock solution to get 10, 20, 30, 40 and 50 µg/ml solutions. The solutions were analysed by UV-Spectrophotometer to find the maximum absorption at a particular wavelength. The  $\lambda_{max}$  was found to be 241 nm. Finally, a graph of absorbance vs concentration was plotted.

## METHODS

### Preparation of nanocrystals<sup>152-154</sup>

Table 1 gives the composition (ratio by weight) of the prepared nanocrystal formulations, using the surfactants sodium lauryl sulphate (SLS) and Tween 80, as well as the polymers HPMC and HPC. The formulations were prepared by sonoprecipitation technique which involves the mixing of 200 mg of drug with 10ml of methanol and the weighed amounts of stabilizers in 10 ml of water. The drug solution is added with the stabilizers which is suspended in water and these suspensions were mixed and sonicated (Elmasonic S 30 H, Germany) for half an hour to break any agglomerated powder. This pre-milling process was followed by exposure to high pressure homogenization (Standsted SPCH-10-Pressure Cell Homogeniser, UK) for 10 cycles at a pressure of 1000 bar. The resulting suspensions were lyophilized (Savant Novalyph-NL500, USA) to obtain dry powder.

### Determination of Drug content

Sample containing 10 mg equivalent of Atorvastatin Calcium nanocrystals are weighed and dissolved in methanol, and the volume is made upto 100ml with phosphate buffer (pH 6.8). From the above solution 10 ml is pipetted out and made upto 100 ml with phosphate buffer (pH 6.8). The absorbance of resulting solution is determined at  $\lambda_{max}$  (241 nm) using Double-beam UV Spectrophotometer (UV-1700 Shimadzu co-operation, Japan) and estimated by its drug content.

## EVALUATION OF PREPARED FORMULATIONS

### Entrapment efficiency:

The nanoparticles were separated from the aqueous medium by ultracentrifugation at 10,000 rpm for 30 min at 5° C. Then the resulting supernatant solution was decanted and dispersed into phosphate buffer (pH 6.8). Thus the procedure was repeated twice to remove the untrapped drug molecules completely. The amount of drug entrapped in the nanoparticles was determined as the difference between the total amount of drug used to prepare the nanoparticles and the amount of drug present in the aqueous medium.

		Amount of drug
released from the lysed nanocrystals		
Entrapment efficiency	(%)	=
x 100		
	Amount of drug initially taken to prepare the nanoparticles	

### Determination of particle size and zeta potential of formulations

Appropriate dilutions of formulations using deionized water were prepared and then these dilutions were examined for their size and zeta potential using a zetasizer (Malvern Zetasizer Nano ZS, UK). The values were compared to those of the drug and a statistical analysis was carried out using a One-Way ANOVA (Post Hoc test used is the LSD) at  $p < 0.05$ , using SPSS 16 program.

### Determination of the saturated solubility of formulation

Saturated solubility of the prepared formulations, the drug as well as the lyophilized drug was determined in water. An excess of the dried powder formulations was suspended in a fixed volume of water and was shaken in a constant temperature water bath (Stuart SBS 40, UK) at 100 rpm at  $37 \pm 0.5^\circ \text{C}$  for 48 h (till equilibrium solubility was attained). At the end of the period, the samples were ultra-centrifuged at 15000 rpm (Megafuge 1.0R, Heraeus, Germany) for 15 min to remove the excess solid, appropriately diluted, and the concentration of atorvastatin was determined by UV spectrophotometry at 241 nm. The concentration of the dissolved atorvastatin was calculated using the equation derived from the built calibration curve of the drug in distilled water. The formulation of the highest solubility was compared to that of a physical mixture of the same drug to stabilizer ratio. The experiment was repeated three times for

each formulation. A statistical analysis was carried out using a One-Way ANOVA at  $p < 0.05$  to compare the results.

#### **In-vitro dissolution studies**

Lyophilized powders, equivalent to 25 mg of atorvastatin were weighted accurately and filled in 00# gelatin capsules. The dissolution rate of pure Atorvastatin nanocrystals were studied in 900 ml of phosphate buffer (pH6.8) using USP type II (Paddle type) dissolution test apparatus with a Paddle stirrer at 50 rpm. A temperature  $37 \pm 0.5^\circ\text{C}$  was maintained throughout the study. Drug or nanocrystals equivalent to 25 mg of Atorvastatin was used in each test. Samples of dissolution media (5ml) were withdrawn through a filter (0.45 $\mu$ ) at different intervals of time, suitably diluted and assayed at 241 nm. The samples of dissolution fluid withdrawn at each time were replaced with 5 ml of fresh fluid. Each formulation was repeated three times. The dissolution profile of the plain drug was also determined, as well as that of the physical mixtures of formulations which possessed the highest dissolution rates. The data of the release experiments obtained at 30 min were compared by determination of the dissolution efficiency (%D.E) and a statistical analysis was run using a One-Way ANOVA test (Post Hoc test: LSD). The dissolution efficiency was calculated according to the following equation.

$$\text{Dissolution efficiency (DE)} = \frac{t_0 y_j}{t y_{100}}$$

$t^* 100$

#### **Release Kinetics:**

Data obtained from *in vitro* release studies were fitted to various kinetic equations. The kinetic models used are zero order equation ( $Q = k_0 t$ ), First order equation  $\{ \ln(100 - Q) = \ln Q - k_1 t \}$ , Higuchi equation ( $Q = k t^{1/2}$ ), Hixson and Crowell model  $Q_t^{1/3}$  Vs  $t$  and  $Q_t^{2/3}$  Vs  $t$  -Modified root cube equation. Further, to find out the mechanism of drug release, first 60% drug release was fitted in Korsmeyer and Peppas equation ( $Q = k p t^n$ ). Where,  $Q$  is the percent of the drug release at time  $t$  and  $k_0$  and  $k_1$  are the coefficients of the equations and  $n$  is the release exponent. The  $n$  value is used to characterize different release mechanism.

#### **Wettability study**<sup>155-157</sup>

The pure drug and formulations were subjected to wettability studies by the Buchner funnel method and water absorption method. In the first method, the pure drug and formulations of about 100 mg were weighed and placed in a Buchner glass funnel. The funnel was plunged into a beaker containing water in a manner that the beaker remains at the same level as the powder in the funnel. Methylene blue powder (100 mg) was layered uniformly on the surface of the powder in the funnel. The time required for wetting methylene blue powder was measured.

#### **Permeation study**<sup>155-157</sup>

The permeation study of the pure drug, and optimized nanocrystal drug was carried out using two different membranes, namely egg membrane and cellulose nitrate membrane. The diffusion of the drug through the membranes was analyzed in a diffusion cell. The required length of membrane was cut and attached to the ground bottom layer of the diffusion cell with glue. The cell (donor compartment) was marked for its 10 ml content and was dipped inside a beaker (receptor compartment) containing phosphate buffer pH 6.8. 10 ml of the buffer was added to the donor compartment. It was noted the level of the buffer inside the cell and in beaker was of same level. Weighed amount of the pure drug and formulations equivalent to specified quantity of the drug was added to the cell. The samples at predetermined time intervals were withdrawn and the same volume of fresh buffer was replaced immediately to maintain sink condition. The study was carried out for 1h. The solutions were suitably diluted and the absorbances were measured using UV spectrophotometer at 241 nm.

For the successful fabrication of a nanocrystal formulation, besides selection of the appropriate excipients, equally important is the characterization of the formulation to ensure that the necessary parameters responsible for the performance of nanocrystals are within the specified limits. The following sections discuss in detail the various characterization tests for the evaluation of nanocrystals.

#### **X-ray Diffraction Analysis, Differential scanning calorimeter (DSC) and Fourier transform infrared spectroscopy (FTIR)**

The formulation that proved to possess the best results in the above investigations was tested for the crystalline properties and compared to atorvastatin calcium powder (XRD, X'pert pro, Pan

Analytical, Netherland) over a range of  $2\theta$  from  $5^\circ$  to  $50^\circ$  with Ni-filtered Cu-K $\alpha$  radiation. The scan speed was  $3^\circ \text{ min}^{-1}$ . Differential scanning calorimetric examinations of both the plain drug and the successful formulation were done. The samples were heated at a constant rate of  $10^\circ\text{C/min}$ , in an atmosphere of nitrogen over a temperature range of  $20\text{--}250^\circ\text{C}$  using DSC-50 (Shimadzu, Kyoto, Japan). Similarly, The IR spectra of the pure drug, the successful formulation and its physical mixture were recorded using Infrared spectrophotometer (Shimadzu IR-345-U-04, Japan).

#### **Scanning electron microscopy**

The best formulation was examined for its surface properties and compared to atorvastatin calcium powder (Jeol-JSM 5200 Scanning Microscope, Japan).

#### **Short-term stability studies**

A short-term stability study was performed on Optimized formulation.. The study was carried out at room temperature and at  $4^\circ\text{C}$  for 7 days. The vials containing ATC nanoparticles suspensions were sealed and wrapped in aluminum foil and subdivided into two groups. One group is stored in refrigerator at  $4^\circ\text{C}$  and the other group is stored at room temperature  $25^\circ\text{C}$  for 7 days. At the predetermined time intervals, aliquots were taken and subjected to particle size and % drug entrapment studies as described above. The change in appearance (presence of aggregates), particle size, span value, and % drug entrapped were recorded and compared to results obtained from freshly prepared nanoparticles.

#### **RESULTS AND DISCUSSION**

##### **UV- Spectra ( $\lambda$ max) of ATC in Phosphate buffer(pH6.8)**

UV- spectra ( $\lambda$  max) of ATC was carried out in Phosphate buffer(pH6.8). The  $\lambda$  max was found to be 241 nm. The UV-spectra is shown in Fig. 1.

##### **Standard Calibration Curve of ATC**

Standard calibration curve of ATC was carried out in Phosphate buffer(pH6.8). The readings from calibration curves in Phosphate buffer(pH6.8) was shown in Table 2 and . Calibration curves in Phosphate buffer(pH6.8) was shown in Fig.2.

##### **Melting Point Determination**

Melting point was determined by using glass capillary method. The melting point of ATC was found to be  $179^\circ\text{C}$ . The obtained nanocrystals were examined according to the previously named tests and the results are given in table no:3.

##### **Particle size and zeta potential**

Size and size distribution are important characterizations of the nanosuspensions because they direct the other properties, such as physical stability, saturation solubility and dissolution velocity, and even clinical efficacy. The smaller the particle size, the higher the surface energy of the particles, which promotes aggregation. The most frequently used techniques for particle size measurements of nanosized systems are dynamic light scattering techniques, static light scattering techniques and microscopy. The mean particle size of nanosuspensions is typically analyzed by dynamic light scattering also known as photon correlation spectroscopy (PCS). It has advantages of yielding accurate results and fast and easy measurement. However, this technique is not feasible to analyze particles larger than  $6\mu$ . Apart from the mean particle diameter, PCS can also yield the width of the particle size distribution, referred to as the "polydispersity index" (PI). The PI value ranges from 0(monodisperse particles) to 0.500 (broad distribution), and is a crucial index that governs the physical stability. For a long-term stability the PI should be as low as possible (Table 4).

##### **Zeta Potential Analysis**

The surface charge of the particles is one of the factors influencing the physical stability of nanosuspensions. The higher the particles are equally charged, greater is the electrostatic repulsion between the particles and greater is the physical stability. The particle surface charge is ideally quantified in terms of the "zeta potential", which is measured via the electrophoretic mobility of the particles in an electric field. The particle charge can be measured in surface charge per unit, determined by colloid titration. The zeta potential is determined by measuring the electrophoretic particle velocity in an electrical field. During the particle movement the diffuse layer is shed off, hence the particle acquires a charge due to the loss of the counter ions in the diffuse

layer. This charge at the border of the shedding is termed as the zeta potential. According to the literature, a zeta potential of at least -30 mV for electrostatic and -20 mV for sterically stabilized systems is desired to obtain a physically stable nanocrystal suspensions. The upper limit for the zeta potential is +30 mV. The investigated nanosuspension showed a value of about  $\pm 33$  mV which indicates good stability of the prepared formulation (Table 4).

The obtained formulations showed the following particle size and zeta potential recorded in Table 6. The nanoparticles showed a significant change in particle size compared to the untreated drug with the exception of formulation 11 which did not significantly differ from the drug. As for statistical analysis of the zeta potential, it was found that the drug has a significantly different zeta potential compared to all formulations.

The permeation study through egg membrane was done as per the method reported by Mehdi Ansari *et al.* and Giovanna Corti *et al.* The data for egg membrane and cellulose nitrate membrane was given in (Table 5). It was observed that the amount of drug permeated in both membranes was found to be higher for the nanocrystals than the pure drug. Permeation through cellulose nitrate membrane shows better result when compared with egg membrane. The results can be considered as the evident for increase in release rate of the drug. The Buchner funnel method and water absorption method for finding out wettability were investigated as per the method reported by M. C. Gohel *et al.* and Sunil Kumar *et al.* respectively and findings are shown in Table 5. The wetting time and water absorption ratio of the pure drug was found to be 80 min, indicating its poor wettability. The wetting time of prepared nanocrystals found to be very less (30 min) than pure drug indicating its higher wettability.

#### Saturated Solubility Determination:

The obtained results for the saturated solubility of the twelve formulations, drug and lyophilized drug are listed in Table 3. It was clear that the saturated solubility of formulation 3 was significantly higher than that of the drug, lyophilized drug, the rest of the formulations as well as its physical mixture at  $P < 0.05$  (Table 6).

Thermodynamic solubility implies the solubility of the most stable crystalline form of the drug in a given medium at a specified pressure and temperature. Solubility can temporarily be higher than the thermodynamic solubility. This may be observed with amorphous forms, metastable polymorphic forms, or nanosized drug particles. This enhanced solubility has been designated with diverse terms, such as kinetic or apparent solubility. Since apparent solubility of nanosized particles is higher than the thermodynamic solubility of the material, dissolution of nanocrystalline material is likely to lead to a supersaturated solution. This is termed as the "spring effect". Eventually, precipitation may sooner or later occur until the concentration is equivalent to the thermodynamic solubility. Furthermore, changes in the composition and pH of the solution such as in the gastrointestinal tract will affect solubility and hence the tendency for crystallization. Therefore, the supersaturated state should be maintained and precipitation hindered to enhance in vivo bioavailability. Some polymers, such as polyvinyl pyrrolidone (PVP), methacrylate co-polymers, hydroxypropyl methylcellulose (HPMC), and hydroxypropyl methylcellulose acetate succinate (HPMC-AS) are effective at maintaining (or at least helping to maintain) supersaturation. This is known as the "Parachute effect".

The parachute effect of the polymer can be due to a combination of mechanisms. First, the polymers can themselves increase the thermodynamic solubility of the drug (also termed as the co-solvency effect), which lowers supersaturation and consequently the thermodynamic driving force for crystallization (this also leads to an additional spring effect with the polymer). Through drug-polymer interaction in solution via electrostatic bonds, van der Waals' forces or hydrogen bonding, even the addition of small amounts of polymers such as PVP and HPMC to solution can significantly increase the aqueous solubility. Second, polymers adsorbed on solid surfaces (e.g., with nanocrystals) can block the interaction of already dissolved drug molecules with crystal surfaces and thereby crystal growth. Electrostatic bonds, van der Waals' forces or hydrogen bonding can all influence the

interaction between the polymer and crystal faces, and therefore the degree of crystal growth inhibition. Moreover, the viscosity of the polymer solution may also inhibit the diffusion of the molecules, which limits crystal growth.

#### Dissolution Studies

The following Figure 4 shows the percentage release from the SLS, Tween 80 and HPMC, HPC formulations, respectively, compared to both the drug, lyophilized drug and the physical mixture of the formulation which showed the highest dissolution rate. The figures showed a significant increase at  $p < 0.05$ , in the percentage of the drug released after 30 min for the nanocrystal formulations (1-12) compared to the drug, the lyophilized drug and the physical mixtures. The lyophilization did not significantly affect the dissolution rate of the drug, where after 120 min the percentage of the drug released did not exceed 32%. The nanocrystal formulations of SLS approached 100% release after ten min. They were also significantly higher compared to that of (drug: SLS 10:1) physical mixture. Tween 80 formulations showed an increase in the percentage released as the amount of added Tween 80 increased in the formulation. As for HPMC and HPC formulations, it was clear that both were superior to the drug and its lyophilized form, yet HPC non significantly improved the dissolution rate compared to HPMC after 30 min from the beginning of the experiment. The formulations also showed an increase in the percentage released compared to the physical mixtures.

Table 8 shows the results for the %D.E. for the plain drug, lyophilized drug, physical mixtures and the twelve formulations. The twelve prepared formulations possessed higher values compared to the plain, lyophilized drugs as well as the physical mixtures. The solid state properties (polymorphic crystal form, solvate (especially hydrate) form, degree of crystallinity) influences the apparent solubility and thereby the dissolution rate. Hence, it is crucial to determine these characteristics in nanocrystals. Ideally, thermodynamically most stable crystalline form is desirable to prevent the peril of solid state transformations during production, storage and/or administration. To increase the dissolution and bioavailability of nanocrystals, it is preferable to formulate the nanocrystals in a metastable crystalline form or even prepare the amorphous equivalent of nanocrystals. However, this is not being practiced commonly.

Different nanocrystal manufacturing conditions and procedures can have an impact on the ensuing solid state form. Furthermore, the environmental conditions affect the thermodynamically stable polymorphic form. For e.g., hydrate forms are generally more stable (and therefore less soluble) in aqueous media. Therefore if the drug is susceptible to hydrate formation, then the potential or factors triggering the said conversion should be extensively investigated during stability studies in different conditions. X-ray powder diffraction (XRD), thermal analytical techniques (differential scanning calorimetry, thermogravimetry, etc.) and vibrational spectroscopy (Infrared and Raman) are the most commonly used methods to determine and monitor the solid state form of nanocrystals.

The data obtained from the first 90% release were fitted to various kinetic equations to determine the mechanism of drug release and release rate as indicated by higher correlation coefficients ( $r^2$ ), the drug release from nanoparticles followed zero order equation and Higuchi model diffusion controlled rather than the first order. Hixson-Crowell and modified cube root equation showed poor correlation. The formulation F3 showed zero order release kinetics, and F11, F14 did not fitted for any other release kinetics. But, release kinetics of F7 indicated that it follow zero order and Higuchi model rather than first order. These findings indicated that the drug release from formulated nanoparticles were diffusion controlled (Table 9)

#### X-Ray Diffraction Analysis

X-ray diffraction studies are usually performed for the confirmation of drug crystallinity following its conversion to a nanocrystal formulation. When X-rays interact with a crystalline substance, a diffraction pattern is obtained. Every crystalline substance gives a specific pattern; the same substance always yields the same pattern; and in a mixture of substances each produces its pattern independently of the others. The X-ray

diffraction pattern of a substance therefore represents the unique fingerprint of the substance.

The following **Figure 5** shows the X-ray diffraction picture of both the drug and formulation 3 which showed an acceptable release pattern and the highest saturation solubility. The Figure shows that both the drug and Formulation 3 exhibited diffraction peaks characteristic for crystalline Atorvastatin Calcium at the  $2\theta$  degree values of 9.37, 11.76, 12.10 and 16.96°. Some additional peaks were observed at  $2\theta$  of 6.0169 and 21.9 for formulation 3. Generally, the intensity of peaks was much decreased for formulation 3. The XRD pattern of pure drug ATC produced several diffraction peaks at  $2\theta$ =17.078 19.43, 21.58 indicating the crystalline nature of ATC. The XRD of nanocrystals exhibited crystallinity with reduced intensity as compared to pure ATC. X-ray diffraction analysis showed retention of the crystalline state of the drug after high pressure homogenization, since the diffraction pattern was preserved. The additional peaks observed for the formulation 3 are characteristic peaks for SLS which is adsorbed on the surface of crystals (32). Also the observed decrease in the intensity of the peaks for formulation 3 was due to the decrease of particle size compared.

#### DSC thermogram

Differential scanning calorimetry (DSC) is one recurrently used method for studying the thermal behaviour of drug and drug nanocrystals. The DSC studies are performed to check the status of crystallinity of drug and interaction of excipients and drug after production of nanocrystals. This is especially important for drugs occurring in different polymorphic forms. Moreover, certain top-down techniques like the high pressure homogenization can lead to particles with an amorphous fraction, thus leading to enhancement of saturation solubility. The DSC of pure drug, physical mixture of drug and excipients (stabilizer) and final formulation which may be in dried form is done. **Figure 6** shows the DSC of both the drug and F3. The drug showed a sharp peak at about 157 °C. For Formulation 3, a peak is observed at 153 °C.

The DSC thermogram of ATC showed an endothermic peak at 172°C, corresponding to its melting point. This peak indicates the crystallinity of ATC. Only one sharp peak was observed which confirmed that ATC is free from impurities. The DSC thermogram of the nanocrystals involving ATC showed endothermic peak at lower temperature i.e 169 °C compared to the peak of pure ATC at 172 °C. This may be attributed to uniform dispersion of ATC into the carrier, maltose. In the DSC, the observed reduction in the endothermic peak of formulation 3 indicates possibly transformation to a more amorphous form of the drug which exhibits polymorphism.

#### FTIR studies

Chemical properties of drug and interaction with excipients are evaluated by FT-IR studies. **Figure 7** shows the FTIR spectroscopic analysis of the drug, formulation 3 and the physical mixture corresponding to formulation 3. The pure drug showed characteristic peaks at 2941  $\text{cm}^{-1}$  (C-H - stretching), 1317  $\text{cm}^{-1}$  (C-N - stretching), 3055  $\text{cm}^{-1}$  (C-HO-stretching alcoholic group), 1651  $\text{cm}^{-1}$  (C = C-bending), 746  $\text{cm}^{-1}$ , 690  $\text{cm}^{-1}$  (C-F-stretching), 1109  $\text{cm}^{-1}$  (O-H-bending) (26). It is clear that the main drug peaks are retained in both the physical mixture as well as the nanocrystals of the drug indicating no possible interaction between the drug and the stabilizer.

#### Scanning electron microscopy

Ideally, the shape or morphology of the nanocrystals can be determined using a transmission electron microscope (TEM) and/or a scanning electron microscope (SEM). A wet sample of suitable concentration is needed for the TEM analysis. When the formulated nanosuspensions are to be converted into a dried powder (e.g., by spray drying or lyophilization), a SEM analysis is crucial to monitor alterations in the particle shape and size before and following the process of the water removal. Principally, agglomeration may be observed following water removal, leading to an increase in the particles size. Such changes and more can be observed through SEM.

The surface morphology before and after the cationic charge nanonization of ATR was examined using scanning electron microscopy. The scanning electron microscopy images of nanocrystal formulations revealed rough scaffold-like structures with high surface area. The particle size was greatly reduced with

smooth surfaces by probe sonication when compared to unmodified ATR or pure drug. The crystals of ATR formulation were different from others and the particles were greatly reduced in size with high surface area indicating multiple scaffold-like structures. This could be the major reason for enhanced aqueous solubility of ATR when compared to other nanocrystal formulations (**Fig:8**)

One of major obstacles that limit the use of nanoparticles is their instability in an aqueous medium and frequently particles aggregation is noticed after long term storage of such systems. Furthermore, drug leakage out of the nanoparticles and non-enzymatic polymer hydrolysis can happen. Formulae F3, F7, F11, and F14 were stored at room temperature and 4 °C for 7 days. Results from particle size analysis showed no significant difference in the particle size for formulae F3 and F11 at room temperature and 4 °C ( $p=0.45$  and  $p=0.08$  respectively) while formulae F11 and F14 showed significantly larger particle size when compared to as before storage ( $p < 0.05$ ) at both temperatures but the increase was higher at room temperature. This could be due to Ostwald ripening which is known to be highly dependent on temperature. Results also showed that the EE was significantly increased after 7 days storage at room temperature for formulae F11 and F14 ( $p < 0.05$ ) while formulae F3 and F7 showed no significant difference in the % drug entrapped. The observed increase in EE is in accordance with published data reporting drug adsorption on the surface of the particle increases as the particle size increases. Table no:10 shows the results obtained from stability studies.

#### CONCLUSION

Drug absorption is directly related to both solubility and permeability and inversely related to lipophilicity. Dissolution from nanocrystals is followed by permeation of the dissolved drug across the gastrointestinal wall (in the same way as drug from a solution formulation). Besides increasing permeation of the drug due to elevated dissolved concentrations, stabilizers present in the formulation themselves interact with cells of the epithelial layers to promote permeation. Hence, Atorvastatin calcium, the lipid lowering agent, is taken as a model drug characterized by poor water solubility and bioavailability. In this study an attempt was made for preparation of nanocrystals using sonoprecipitation method. A number of stabilizers were included as well as polymers at different concentrations, and the formulations were homogenized for ten cycles at a pressure of 1000 bars. The obtained nano crystals were evaluated by determining their size, zeta potential, saturated solubility and dissolution rate. Results revealed that Formulation 3, containing (10: 1) drug to sodium lauryl sulphate ratio, possessed the highest saturated solubility and dissolution rate, and hence was analyzed by X-ray diffraction analysis, differential scanning calorimetry, Fourier transform infrared spectroscopy and scanning electron microscopy. The increase in drug dissolution rate and solubility can be expected to have a significant impact on the oral bioavailability of the drug. This study demonstrated the usefulness of the sonoprecipitation technique as a method of enhancing the dissolution of poorly soluble drug-like AC (Atorvastatin Calcium).

#### REFERENCES

1. Natarajan, K., Gajendran, P.L., Arjunkumar, R., Rajesh Kumar, S. Anti-fungal activity of chitosan nanoparticle incorporated lycopene against *Candida albicans* using minimal inhibitory concentration assay 2020 Plant Cell Biotechnology and Molecular Biology 21-232
- Preeti, R., Anitha, R., Rajeshkumar, S., Lakshmi, T. Anti-diabetic activity of silver nanoparticles prepared from cumin oil using alpha amylase inhibitory assay 2020 International Journal of Research in Pharmaceutical Sciences Issue 11,2
- Sathvika, K., Rajeshkumar, S., Lakshmi, T., Roy, A. Anti-fungal activity of selenium nanoparticles synthesized using *symplocos racemosa* against *candida albicans* 2020 Plant Cell Biotechnology and Molecular Biology 21 ;27-28

- Cibikkarthik, T., Rajeshkumar, S., Lakshmi, T., Roy, A. Anti-inflammatory activity of avocado seed extract mediated silver nanoparticles 2019 Drug Invention Today Issue 9
- Mohamed Thamemul Ansari, K.A., Roy, A., Rajeshkumar, S. Anti-inflammatory activity of cinnamon oil mediated silver nanoparticles -An in vitro study 2019 International Journal of Research in Pharmaceutical Sciences Issue 10, 4
- Maajida Aafreen, M., Anitha, R., Preethi, R.C., Rajeshkumar, S., Lakshmi, T. Anti-inflammatory activity of silver nanoparticles prepared from ginger oil-an invitro approach 2019 Indian Journal of Public Health Research and Development, Issue 10, 7
- 7.Vaishnavi Devi, B., Rajeshkumar, S., Lakshmi, T., Roy, A. Anti-inflammatory activity of silver nanoparticles synthesised using *Andrographis paniculata* and *Phyllanthus niruri* 2020 Plant Cell Biotechnology and Molecular Biology 21 25-26
- 8.Chithralekha, B., Rajeshkumar, S., Lakshmi, T., Roy, A. Anti-inflammatory activity of silver nanoparticles synthesized using neem and Aloe vera extract 2019 Drug Invention Today 12 7
- 9.Lab, A.K., Rajasekar, A., Rajeshkumar, S. Anti-inflammatory activity of titanium dioxide nanoparticles synthesised using grape seed extract: An in vitro study 2020 Plant Cell Biotechnology and Molecular Biology 21 2324
- 10.Rajkumar, K.V., Jothipriya, A., Arivarasu, L., Kumar, R., Devi, G. Anti-inflammatory activity of tulasi and turmeric mediated copper nanoparticles 2020 Plant Cell Biotechnology and Molecular Biology 21 47-48
- 11.Das, A., Roy, A., Rajeshkumar, S., Lakshmi, T. Anti-inflammatory activity of turmeric oil mediated silver nanoparticles 2019 Research Journal of Pharmacy and Technology 12 7
- 12.Rangeela, M., Rajeshkumar, S., Lakshmi, T., Roy, A. Anti-inflammatory activity of zinc oxide nanoparticles prepared using amla fruits 2019 Drug Invention Today 11 10
- 13.Wadhwa, R., Paudel, K.R., Chin, L.H., Hon, C.M., Madheswaran, T., Gupta, G., Panneerselvam, J., Lakshmi, T., Singh, S.K., Gulati, M., Dureja, H., Hsu, A., Mehta, M., Anand, K., Devkota, H.P., Chellian, J., Chellappan, D.K., Hansbro, P.M., Dua, K. Anti-inflammatory and anticancer activities of Naringenin-loaded liquid crystalline nanoparticles in vitro 2020 Journal of Food Biochemistry
- 14.Francis, T., Rajeshkumar, S., Roy, A., Lakshmi, T. Anti-inflammatory and cytotoxic effect of arrow root mediated selenium nanoparticles 2020 Pharmacognosy Journal 12 6
- Dharahaas, C., Geetha, R.V. Antibacterial action of bio nanoparticles on *Streptococcus* mutants and *Enterococcus faecalis* - An in vitro study 2018 Drug Invention Today 10 12
- 16.Soundarajan, S., Malaippan, S., Rajeshkumar, S. Antibacterial activity and cytotoxicity of amla seed mediated graphene oxide, silver nanoparticle & Go-Ag nanoparticle - an in vitro study 2020 Plant Cell Biotechnology and Molecular Biology 21 51-52
- Cinthura, C., Rajasekar, A. Antibacterial activity of cinnamon - Clove mediated silver nanoparticles against *Streptococcus mutans* 2020 Plant Cell Biotechnology and Molecular Biology 21 31-32
- Bharathi, R., Rajasekar, A., Rajeshkumar, S. Antibacterial activity of grape seed mediated ZnO nanoparticles against *Lactobacillus* species and *Streptococcus mutans* 2020 Plant Cell Biotechnology and Molecular Biology 21 35-36
- Malaikolundhan, H., Mookkan, G., Krishnamoorthi, G., Matheswaran, N., Alsawalha, M., Veeraraghavan, V.P., Krishna Mohan, S., Di, Anticarcinogenic effect of gold nanoparticles synthesized from *Albizia lebbek* on HCT-116 colon cancer cell lines 2020 :Artificial Cells, Nanomedicine and Biotechnology 48-1
- Han, X., Jiang, X., Guo, L., Wang, Y., Veeraraghavan, V.P., Krishna Mohan, S., Wang, Z., Cao, D. Anticarcinogenic potential of gold nanoparticles synthesized from *Trichosanthes kirilowii* in colon cancer cells through the induction of apoptotic pathway 2019 Artificial Cells, Nanomedicine and Biotechnology 47 1
- Sree Vidhya, T.M., Geetha Antimicrobial effects of bionanoparticles 2014 Research Journal of Pharmacy and Technology 7 3
- Sangeetha, K., Alsharani, F.A., Angelin Vinodhini, P., Sudha, P. N., Jayachandran, V., Sukumaran, A. Antimicrobial efficacy of novel nanochitosan-based mat via electrospinning technique 2018 Polymer Bulletin 75 12
- Haripriya, S., Ajitha, P. Antimicrobial efficacy of silver nanoparticles of Aloe vera 2017 Journal of Advanced Pharmacy Education and Research 7 2
- Li, Z., Veeraraghavan, V.P., Mohan, S.K., Bolla, S.R., Lakshmanan, H., Kumaran, S., Aruni, W., Aladresi, A.A.M., Shair, O.H.M., Alharbi, S.A., Chinnathambi, A. Apoptotic induction and anti-metastatic activity of eugenol encapsulated chitosan nanopolymer on rat glioma C6 cells via alleviating the MMP signaling pathway 2020 Journal of Photochemistry and Photobiology B: Biology 203
- Sneha, B. Application of nanotechnology in dentistry 2014 Research Journal of Pharmacy and Technology
- Anvesh, P., Madhu, S. Applications of carbon nano tubes (CNT) in automobiles - A review 2015 International Journal of Applied Engineering Research 10-33
- Gomathi, M., Prakasam, A., Chandrasekaran, R., Gurusubramaniam, G., Revathi, K., Rajeshkumar, S. Assessment of Silver Nanoparticle from *Cocos nucifera* (coconut) Shell on Dengue Vector Toxicity, Detoxifying Enzymatic Activity and Predatory Response of Aquatic Organism 2019 Journal of Cluster Science 30-6
- Rajeshkumar, S., Sandhiya, D. Biomedical applications of zinc oxide nanoparticles synthesized using eco friendly method 2020 Nanoparticles and their Biomedical
- Revathi, B., Rajeshkumar, S., Roy, A., Lakshmi, T. Biosynthesis of copper oxide nanoparticles using herbal formulation and its characterisation 2019 International Journal of Research in Pharmaceutical Sciences 10-3
- Shreelakshmi, S., Doraiakannan, S., Indiran, I.M.A., Rajeshkumar, S. Bleaching efficacy of carbamide peroxide, fluoridated carbamide peroxide against nanohydroxyapatite reinforced carbamide peroxide-an in vitro study 2019 Indian Journal of Public Health Research and Development 10-11
- Karthikeyan et al., Saveetha institute of Medical and Technical Sciences, A revised analysis of current and emerging Nano suspension technological approaches for cardiovascular medicine December 2022, Beni-Suef University Journal of Basic and Applied Sciences, 2022(11-10)
- Magdalene R. Pure drug nanoparticles for the formulation of poorly soluble drugs. *New Drugs* 2001;3:62-68.
- Moschitz J, Muller RH. Drug nanocrystals the universal formulation approach for poorly soluble drugs. In: Thassu D, Deleers M, Pathak Y, editors. Nanoparticulate drug delivery systems. New York: Informa Healthcare; 2007. Pg no.: 71-88.
- Gao L, Zhang D, Chen M. Drug nanocrystals for the formulation of poorly soluble drugs and its application as a potential drug delivery system. *J Nanopart Res* 2008; 10:845-862.
- Junghanns JUAH, Muller RH. Nanocrystal technology, drug delivery and clinical applications. *Int J Nanomedicine* 2008;3(3):295-309.

- Chen H, Khemtong C, Yang X, et al. Nanonization strategies for poorly water-soluble drugs. *Drug Discovery Today* 2011; 16(7/8):354-360.
- Muller RH, Gohla S, Keck CM. State of the art of nanocrystals e special features, production, nanotoxicology aspects and intracellular delivery. *Eur J Pharm Biopharm* 2011; 78:1-9.
- Kocbek P, Baumgartner S, Kristl J. Preparation and evaluation of nanosuspensions for enhancing the dissolution of poorly soluble drugs. *Int J Pharm* 2006; 312:179-186.
- Sinha B, Muller RH, Moschwitz JP. Bottom-up approaches for preparing drug nanocrystals: formulations and factors affecting particle size. *Int J Pharm* 2013; 453:126-141.
- Moschwitz JP. Drug nanocrystals in the commercial pharmaceutical development process. *Int J Pharm* 2013; 453:142-156.
- Keck CM, Muller RH. Drug nanocrystals of poorly soluble drugs produced by high pressure homogenisation. *Eur J Pharm Biopharm* 2006; 62:3-16.
- Merisko-Liversidge E, Liversidge GG. Nanosizing for oral and parenteral drug delivery: a perspective on formulating poorly-water soluble compounds using wet media milling technology. *Adv Drug Deliv Rev* 2011; 30:427-440.
- Eerdenbrugh BV, den Mooter GV, Augustijns P. Top-down production of drug Nanocrystals: nanosuspension stabilization, miniaturization and transformation into solid products. *Int J Pharm* 2008; 364-75.
- Niwa T, Miura S, Danjo K. Universal wet-milling technique to prepare oral nanosuspension focused on discovery and preclinical animal studies e development of particle design method. *Int J Pharm* 2011; 405:218-227.
- Merisko-Liversidge E, Liversidge GG. Drug nanoparticles: formulating poorly water-soluble compounds. *Toxicol Pathol* 2008; 36(1):43-48.
- Bushrab FN, Muller RH. Nanocrystals of poorly soluble drugs for oral administration. *New Drugs* 2003; 5:20-22.
- Morakul B, Suksiriworapong J, Leanpolchareanchai J, et al. Precipitation-lyophilization-homogenization (PLH) for preparation of clarithromycin nanocrystals: influencing factors on physicochemical properties and stability. *Int J Pharm* 2013; 457:187-196.
- Liversidge GG, Cundy KC. Particle size reduction for improvement of oral bioavailability of hydrophobic drugs: I. Absolute oral bioavailability of nanocrystalline danazol in beagle dogs. *Int J Pharm* 1995; 125(1):91-97.
- Kesisoglou F, Mitra A. Crystalline nanosuspensions as potential toxicology and clinical oral formulations for BCS II/ IV compounds. *AAPS J* 2012; 14:677-687.
- Peters K, Leitzke S, Diederichs JE, et al. Preparation of a clofazimine nanosuspension for intravenous use and evaluation of its therapeutic efficacy in murine *Mycobacterium avium* infection. *J Antimicrob Chemotherapy* 2000; 45(1):77-83.
- Ganta S, Paxton JW, Baguley BC, et al. Formulation and pharmacokinetic evaluation of an Asulacrine nanocrystalline suspension for intravenous delivery. *Int J Pharm* 2009; 367: 179-186.
- Rosario P, Claudio B, Ferrara P, et al. Eudragit RS100 nanosuspensions for the ophthalmic controlled delivery of ibuprofen. *Eur J Pharm Sci* 2002; 16:53-61.
- Kassem MA, Abdel Rahman AA, Ghorab MM, et al. Nanosuspension as an ophthalmic Delivery system for certain glucocorticoid drugs. *Int J Pharm* 2007; 340:126-133.
- Ali HSM, York P, Ali AMA, et al. Hydrocortisone nanosuspensions for ophthalmic delivery: a comparative study between microfluidic nanoprecipitation and wetmilling. *J of Control Release* 2011; 149:175-181.
- Jacobs C, Muller RH. Production and characterization of a budesonide nanosuspension for pulmonary administration. *Pharm Res* 2002; 19(2):189-194.
- Sultana S, Talegaonkar S, Ali R, et al. Inhalation of alendronate nanoparticles as dry powder inhaler for the treatment of osteoporosis. *J Microencapsulation* 2012; 29 (5): 445-454.
- Zhang J, Lv H, Jiang K, et al. Enhanced bioavailability after oral and pulmonary administration of baicalein nanocrystal. *Int J Pharm* 2011; 420:180-188.
- Shaal LA, Shegokar R, Muller RH. Production and characterization of antioxidant Apigenin nanocrystals as a novel UV skin protective formulation. *Int J Pharm* 2011; 420:133-140.
- Mitri K, Shegokar R, Gohla S, et al. Lutein nanocrystals as antioxidant formulation for oral and dermal delivery. *Int J Pharm* 2011; 420:141-146.
- Zhai X, Lademann J, Keck CM, et al. Nanocrystals of medium soluble actives novel: Concept for improved dermal delivery and production strategy. *Int J Pharm* 2014; 470: 141 -150.
- Mishra PR, Shaal LA, Muller RH, et al. Production and characterization of hesperetin nanosuspensions for dermal delivery. *Int J Pharm* 2009; 371:182-189.
- Kayser O, Olbrich C, Yardley V, et al. Formulation of amphotericin B as nanosuspension for oral administration. *Int J Pharm* 2003; 254:73-75.
- Liversidge GG, Conzentino P. Drug particle size reduction for decreasing gastric irritancy and enhancing absorption of naproxen in rats. *Int J Pharm* 1995; 125:309-313.
- Li W, Yang Y, Tian Y, et al. Preparation and in vitro/in vivo evaluation of revaprazan Hydrochloride nanosuspension. *Int J Pharm* 2011; 408:157-162.
- Xia D, Quan P, Piao H, et al. Preparation of stable nitrendipine nanosuspensions using the precipitation - ultrasonication method for enhancement of dissolution and oral bioavailability. *Eur J Pharm Sci* 2010; 40:325-334.
- Kayser O. A new approach for targeting to *Cryptosporidium parvum* using mucoadhesive nanosuspensions: research and applications. *Int J Pharm* 2001; 214:83-85.
- Jinno J, Kamada N, Miyake M, et al. Effect of particle size reduction on dissolution and oral absorption of a poorly water-soluble drug, cilostazol, in beagle dogs. *J Control Release* 2006; 111:56-64.
- Wu Y, Loper A, Landis E, et al. The role of biopharmaceutics in the development of a clinical nanoparticle formulation of MK-0869: a Beagle dog model predicts improved bioavailability and diminished food effect on absorption in human. *Int J Pharm* 2004; 285:135-146.
- Sauron R, Wilkins M, Jessent V, et al. Absence of a food effect with a 145 mg nanoparticle fenofibrate tablet formulation. *Int J Clin Pharmacol Ther* 2006; 44(2): 64-70.
- Kirkof N. Creation and characterization of nanoparticles. In: 32<sup>nd</sup> annual meeting and Exposition of the controlled release society Miami; 2005.
- Moschwitz J, Muller RH. From the drug nanocrystals to the final mucoadhesive oral Dosage form; 2004.
- Moschwitz J, Muller RH. Spray coated pellets as carrier system for mucoadhesive drug nanocrystals. *Eur J Pharm Biopharm* 2006; 62(3):282-287.
- Moschwitz J, Muller RH. Controlled drug delivery system for oral application of drug nanocrystals. 2004 AAPS annual meeting and exposition. Baltimore: MD; 2004.
- Food and drug administration, Center for drug evaluation and research. Orange book: Approved drug products with therapeutics equivalence evaluations.

- De Waard H, Frijlink HW, Hinrichs WL. Bottom up preparation techniques for nanocrystals of lipophilic drugs. *Pharm Res* 2011; 28:1220-1223.
- Vergote GJ, Vervaet C, Driessche IV, et al. In vivo evaluation of matrix pellets containing nanocrystalline ketoprofen. *Int J Pharm* 2002; 240:79-84.
- Muller RH, Runge S, Revelli V, et al. Oral bioavailability of cyclosporine: solid lipid nanoparticles (SLN) versus drug nanocrystals. *Int J Pharm* 2006; 317:82-89.
- Lungguth P, Hanafy A, Frenzel D, et al. Nanosuspension formulations for low-soluble drugs: pharmacokinetic evaluation using spironolactone as model compound. *Drug Dev Ind Pharm* 2005; 31:319-329.
- Mou D, Chen H, Wan J, et al. Potent dried drug nanosuspensions for oral bioavailability enhancement of poorly soluble drugs with pH-dependent solubility. *Int J* 2011; 413:237-244.
- Haines, P.; Reading, M.; Wilburn, F. Differential thermal analysis and differential scanning calorimetry. In *Handbook of Thermal Analysis and Calorimetry*; Brown M.E., Ed.; Elsevier Science: Amsterdam, The Netherlands, 1998; pp. 279-361.
- Danley, R. New heat flux DSC measurement technique. *Thermochim. Acta* 2002, 395, 201-208. [CrossRef]
- Zucca, N.; Erriu, G.; Onnis, S.; Longoni, A. An analytical expression of the output of a power compensated DSC in a wide temperature range. *Thermochim. Acta* 2002, 143, 117-125. [CrossRef]
- Kocbek, P.; Baumgartner, S.; Kristl, J. Preparation and evaluation of nanosuspensions for enhancing the dissolution of poorly soluble drugs. *Int. J. Pharm.* 2006, 312, 179-186. [CrossRef] [PubMed]
- Yin, S.; Franchini, M.; Chen, J.; Hsieh, A.; Jen, S.; Lee, T.; Hussain, M.; Smith, R. Bioavailability enhancement of a COX-2 inhibitor, BMS-347070, from a nanocrystalline dispersion prepared by spray-drying. *J. Pharma. Sci.* 2005, 94, 1598-1607. [CrossRef] [PubMed]
- Huang, Y.; Luo, X.; You, X.; Xia, Y.; Song, X.; Yu, L. The preparation and evaluation of water-soluble b610 nanosuspensions with improved bioavailability. *AAPS PharmSciTech* 2013, 14, 1236-1243. [CrossRef] [PubMed]
- Koneti, V.; Singh, S.K.; Gulati, M. A comparative study of top-down and bottom-up approaches for the preparation of nanosuspensions of glipizide. *Powder Technol.* 2014, 256, 436-449.
- Liandong, H.; Dongqian, K.; Qiaofeng, H.; Na, G.; Saixi, P. Evaluation of high-performance curcumin nanocrystals for pulmonary drug delivery both in vitro and in vivo. *Nanoscale Res. Lett.* 2015, 10. [CrossRef]
- De Waard, H.; De Beer, T.; Hinrichs, W.; Vervaet, C.; Remon, J.; Frijlink, H. Controlled crystallization of the lipophilic drug fenofibrate during freeze-drying: Elucidation of the mechanism by in-line Raman spectroscopy. *AAPS J.* 2010, 12, 569-575. [CrossRef] [PubMed]
- Ali, H.; York, P.; Ali, A.; Blagden, N. Hydrocortisone nanosuspensions for ophthalmic delivery: A comparative study between microfluidic nanoprecipitation and wet milling. *J. Control. Release* 2011, 149, 175-181. [CrossRef] [PubMed]
- Lai, F.; Pini, E.; Corrias, F.; Perricci, J.; Manconi, M.; Fadda, A.M.; Sinico, C. Formulation strategy and evaluation of nanocrystal piroxicam orally disintegrating tablets manufacturing by freeze-drying. *Int. J. Pharm.* 2014, 467, 27-33. [CrossRef] [PubMed]
- Pireddu, R.; Sinico, C.; Ennas, G.; Marongiu, F.; Muzzalupo, R.; Lai, F.; Fadda, A. Novel nanosized formulations of two diclofenac acid polymorphs to improve topical bioavailability. *Eur. J. Pharm. Sci.* 2015, 77, 208-215. [CrossRef] [PubMed]
- Keck, C.; Muller, R. Characterisation of nanosuspensions by laser diffractometry. In *Proceedings of the Annual Meeting of the American Association of Pharmaceutical Scientists (AAPS)*, Nashville, TN, USA, 6-10 November 2005.
- Bott, S.; Hart, W. Particle Size Analysis Utilizing Polarization Intensity Differential Scattering. U.S. Patent 4,953-978, 1990.
- Xu, R. Extracted Polarization Intensity Differential Scattering for Particle Characterization. U.S. Patent 6,859-276, 2003.
- Keck, C.; Müller, R. Particle size analysis with laser diffractometry is not sensitive enough to detect changes in a lipid carrier system. In *Proceedings of the Annual Meeting of the American Association of Pharmaceutical Scientists (AAPS)*, Nashville, TN, USA, 6-10 November 2005.
- Gao, L.; Zhang, D.; Chen, M. Drug nanocrystals for the formulation of poorly soluble drugs and its application as a potential drug delivery system. *J. Nanopart. Res.* 2008, 10, 845-862. [CrossRef]
- Rawle, A. Nanopowders—An oxymoron. In *Proceedings of the Particles 2004—Particle Synthesis, Characterization, and Particle-Based Advanced Materials*, Orlando, FL, USA, 6-9 March 2004.
- Moribe, K.; Wanawongthai, C.; Shudo, J.; Higashi, K.; Yamamoto, K. Morphology and surface states of colloidal probucol nanoparticles evaluated by atomic force microscopy. *Chem. Pharm. Bull.* 2008, 56, 878-880. [CrossRef] [PubMed]
- Liu, P.; Viitala, T.; Kartal-Hodzig, A.; Liang, H.; Laaksonen, T.; Hirvonen, J.; Peltonen, L. Interaction studies between indomethacin nanocrystals and PEO/PPO copolymer stabilizers. *Pharm. Res.* 2015, 32, 628-639. [CrossRef] [PubMed]
- Hassan, M.S.; Lau, R.W.M. Effect of particle shape on dry particle inhalation: Study of flowability, aerosolization, and deposition properties. *AAPS PharmSciTech* 2009, 10, 1252-1262. [CrossRef] [PubMed]
- Li, Y.; Dong, L.; Jia, A.; Chang, X.; Xue, H. Preparation and characterization of solid lipid nanoparticles loaded traditional Chinese medicine. *Int. J. Biol. Macromol.* 2006, 38, 296-299. [CrossRef] [PubMed] [Pharmaceutics 2016].
- Ige, P.; Baria, R.; Gattani, S. Fabrication of fenofibrate nanocrystals by probe sonication method for enhancement of dissolution rate and oral bioavailability. *Colloids Surf. B* 2013, 108, 366-373. [CrossRef] [PubMed]
- Sarnes, A.; Stergaard, J.; Smedegaard Jensen, S.; Aaltonen, J.; Rantanen, J.; Hirvonen, J.; Peltonen, L. Dissolution study of nanocrystal powders of a poorly soluble drug by UV imaging and channel flow methods. *Eur. J. Pharm. Sci.* 2013, 50, 511-519. [CrossRef] [PubMed]
- Frank, K.; Westedt, U.; Rosenblatt, K.; Hölig, P.; Rosenberg, J.; Mägerlein, M.; Fricker, G.; Brandl, M. What is the mechanism behind increased permeation rate of a poorly soluble drug from aqueous dispersions of an amorphous solid dispersion? *J. Pharm. Sci.* 2014, 103, 1779-1786. [CrossRef] [PubMed]
- Surwase, S.; Itkonen, L.; Aaltonen, J.; Saville, D.; Rades, T.; Peltonen, L.; Strachan, C. Polymer incorporation method affects the physical stability of amorphous indomethacin in aqueous suspension. *Eur. J. Pharm. Biopharm.* 2015, 96, 32-43. [CrossRef] [PubMed]
- Ghosh, I.; Bose, S.; Vippagunta, R.; Harmon, F. Nanosuspension for improving the bioavailability of a poorly soluble drug and screening of stabilizing agents to inhibit crystal growth. *Int. J. Pharm.* 2011, 409, 260-268. [CrossRef] [PubMed]
- Ueda, K.; Higashi, K.; Yamamoto, K.; Moribe, K. In situ molecular elucidation of drug supersaturation achieved by nano-sizing and amorphization of poorly water-soluble drug. *Eur. J. Pharm. Sci.* 2015, 77, 79-89. [CrossRef] [PubMed]



- Rabinow, B. Nanosuspensions in drug delivery. Nat. Rev. Drug Discov. 2004, 3, 785-796. [CrossRef] [PubMed]
- Patzelt, A.; Richter, H.; Knorr, F. Selective follicular targeting by modification of the particle sizes. J. Control. Release 2011, 150, 45-48. [CrossRef] [PubMed]
- Lademann, J.; Richter, H.; Teichmann, A. Nanoparticles—An efficient carrier for drug delivery into the hair follicles. Eur. J. Pharm. Biopharm. 2007, 66, 159-164. [CrossRef] [PubMed]
- Lang, J.; Roehrs, R.; Jani, R. Ophthalmic Preparations. In Remington: The Science and Practice of Pharmacy; Lippincott Williams & Wilkins: Philadelphia, PA, USA, 2006.
- Franz, T. Percutaneous absorption on the relevance of in vitro data. J. Investig. Dermatol. 1975, 64, 190-195. [CrossRef] [PubMed]
- Bronaugh, R.; Stewart, R. Methods for in vitro percutaneous absorption studies IV: The flow-through diffusion cell. J. Pharm. Sci. 1985, 74, 64-67. [CrossRef] [PubMed]
- Brain, K.; Walters, K.; Watkinson, A. Dermal Absorption and Toxicity Assessment; Roberts, M.S., Walter, K.A., Eds.; Marcel Dekker Inc.: New York, NY, USA, 1998; pp. 161-187.
- Li, W.; Quan, P.; Zhang, Y.; Cheng, J.; Liu, J.; Cun, D.; Xiang, R.; Fang, L. Influence of drug physicochemical properties on absorption of water insoluble drug nanosuspensions. Int. J. Pharm. 2014, 460, 13-23. [CrossRef] [PubMed]
- Guo, Y.; Luo, J.; Tan, S.; Otieno, B.O.; Zhang, Z. The applications of vitamin E TPGS in drug delivery. Eur. J. Pharm. Sci. 2013, 49, 175-186. [CrossRef] [PubMed]
- Chen, Y.; Li, T. Cellular uptake mechanism of paclitaxel nanocrystals determined by confocal imaging and kinetic measurement. AAPS J. 2015, 17, 1126-1134. [CrossRef] [PubMed]
- Gao, L.; Liu, G.; Ma, J.; Wang, X.; Wang, F.; Wang, H.; Sun, J. Paclitaxel nanosuspension coated with P-gp inhibitory surfactants: II. Ability to reverse the drug-resistance of H460 human lung cancer cells. Colloids Surf. B 2014, 117, 122-127.
- Strachan, C.; Rades, T.; Gordon, K.; Rantanen, J. Raman spectroscopy for quantitative analysis of pharmaceutical solids. J. Pharm. Pharmacol. 2007, 59, 179-192. [CrossRef] [PubMed]
- Darville, N.; van Heerden, M.; Vynckier, A.; de Meulder, M.; Sterkens, P.; Annaert, P.; van den Mooter, G. Intramuscular administration of paliperidone palmitate extended-release injectable microsuspension induces a subclinical inflammatory reaction modulating the pharmacokinetics in rats. J. Pharm. Sci. 2014, 103, 2072-2087. [CrossRef] [PubMed]
- Samtani, M.; Vermeulen, A.; Stuyckens, K. Population pharmacokinetics of intramuscular paliperidone palmitate in patients with schizophrenia: A novel once-monthly, long-acting formulation of an atypical antipsychotic. Clin. Pharmacokinet. 2009, 48, 585-600. [CrossRef] [PubMed]
- Fessi H, Dalencon F, Amjaud Y, Lafforge C, Derouin F. Atovaquone and Rifabutin Loaded nanocapsules: formulation studies. Int J Pharm. 1997, 153: 127-130.
- Jacobs C, Kayser O, Muller RH. Nanosuspensions as a new approach for the formulation for the poorly soluble drug tarazepide. Int J Pharm. 2000, 196: 161-164.
- Trotta M, Debernardi F, Caputo O. Preparation of solid lipid nanoparticles by a solvent emulsification-diffusion technique. Int J Pharm. 2003, 257: 153-160.
- Jiang B, Hu L, Gao C, Shen J. Ibuprofen-loaded nanoparticles prepared by a coprecipitation method and their release properties. Int J Pharm. 2005, 304: 220-230.
- Hecq J, Deleers M, Fanara D, Vranckx H, Amighi K. Preparation and
- Characterization of nanocrystals for solubility and dissolution rate enhancement of Nifedipine. Int J Pharm. 2005, 299: 167-177.
- Amighi, K., Hecq, J., Deleers, M., Fanara, D., Vranckx, J. 2005. Preparation and characterization of nanocrystals for solubility and dissolution rate enhancement of Nifedipine. Int. J. Pharm, 299, 167-177.
- Jonghwi Lee., Ji-Yeun Choi., Ji Youn Yoo., Hae-Soo Kwak., Byeong Uk Nam., 2005. Role of polymeric stabilizers for drug nanocrystal dispersions, J. Current Applied Physics, 5, 472-474.
- J. Hecqa, M. Deleers, D Fanara, K. Amighi, 2005., Preparation and characterisation of nanocrystals for solubility and dissolution rate enhancement of Nifedipine; International Journal Of Pharmaceutics 299(2005) 167-177.
- Dillen K, Vandervoort J, Van den Mooter G, Ludwig A. Evaluation of ciprofloxacin loaded Eudragit RS100 or RL100/PLGA nanoparticles. Int J Pharm. 2006, 314: 72-82.
- Hecq J, Deleers M, Fanara D, Vranckx H, Boulanger P, Le Lamer S, Amighi. Preparation and in vitro/in vivo evaluation of nano-sized crystals for dissolution rate enhancement of ucb-35440-3, a highly dosed poorly water-soluble weak base. Eur J Pharm Biopharm. 2006, 64: 360-368.
- Rainer Muller, H., Cornelia Keck, M., 2006. Drug nanocrystals of poorly soluble drugs produced by high pressure homogenization, Eur. J. Pharm. Biopharm, 62, 3-16

#### TABLES

Table 1: Composition of the Prepared Nanoparticle Formulations

Formulation	Composition
1	20: 1 Drug :SLS
2	15: 1 Drug :SLS
3	10: 1 Drug :SLS
4	5: 1 Drug :SLS
5	20:1 Drug: Tween 80
6	15:1 Drug: Tween 80
7	10:1 Drug: Tween 80
8	5:1 Drug: Tween 80
9	1:1 HPMC : Drug
10	0.5:1 HPMC : Drug
11	1:1 HPC: Drug
12	0.5:1 HPC: Drug

SLS: Sodium lauryl sulphate; HPMC: hydroxypropyl methyl cellulose;  
HPC: hydroxypropyl cellulose

Table 2: Readings from Calibration Curve in Phosphate Buffer (pH 6.8)

Concentration (µg/ml)	Absorbance (at 241 nm)
5	0.212
10	0.422
15	0.612
20	0.805
25	1.015

Table 3: Drug Content and Entrapment Efficiency of Prepared Nanocrystals

Sl No	Formulation Code	Drug Content	Entrapment Efficiency
1.	F1	74.43	39.02
2.	F2	76.21	40.18
3.	F3	78.01	52.04
4.	F4	80.25	54.10
5.	F5	67.65	12.46
6.	F6	65.23	22.45
7.	F7	62.10	14.50
8.	F8	60.72	25.20
9.	F9	89.04	58.52
10.	F10	90.48	63.45
11.	F11	93.72	74.20
12.	F12	91.02	66.56
13.	F13	83.50	44.20
14.	F14	79.43	48.32
15.	F15	86.58	51.22
16.	F16	88.53	62.31

Table 4: Particle Size and Zeta Potential Values of Prepared Formulations Compared to the Drug

Formulation	Particle size (nm)	Zeta potential (mv)
1	583.7(±11.3)	-24.8(±1.5)
2	574.2(±10.04)	-23.2(±0.141)
3	546.1(±11)	-25.7(±0.42)
4	593.1(±9.26)	-26.2(±0.9)
5	611(±6.36)	-7.52(±0.97)
6	539.2(±10.04)	-26.1(±0.97)
7	502.5(±2.47)	-25.4(±1.48)
8	231.7(±12.9)	-27.9(±1.6)
9	931.9(±12.09)	-11.4(±0.63)
10	1404(±10.6)	-3.56(±1.08)
11	709.6(±7.35)	-11.1(±0.6)
12	970.2(±0.46)	-12.4(±0.29)
Drug	708.4(±8.2)	-15.4(±3.1)

Table 5: Permeability and wettability data

Formulation	Permeability (mg/ml/h)		Wettability
	Egg membrane	Cellulose nitrate membrane	Buchner Funnel Method (min)
PureDrug	0.0030	0.0137	80±0.5
Optimized formulation	0.0103	0.0328	30±0.2

Table 6: Saturated Solubility of Formulations

Formulation	Saturated Solubility (µg/mL)
F1	78.55(±2.97)
F2	93.28(±12.9)
F3	383.95(±4.27)
F4	383.95(±4.27)
F5	79.98(±1.43)
F6	182.78(±3.82)
F7	73.16(±1.29)
F8	76.14(±2.02)
F9	79.25(±6.89)
F10	60.35(±1.66)
F11	71.18(±1.28)
F12	78.75(±0.87)
puredrug	43.67(±4.24)
Lyophilized drug	68.804(±0.85)
Physical Mixture of F3	154.294 (±0.71)

Table 8: Dissolution Efficiency of Nanocrystal Formulations Compared to the Plain Drug

Formulation	% D.E.
1	33.791
2	29.881
3	30.399
4	24.567
5	25.647
6	18.246
7	33.727
8	36.358
9	30.411
10	29.106
11	25.669
12	25.125
Drug	11.095
Lyophilized drug	7.418
Physical mixture of Formulation 03	15.073
Physical mixture of Formulation 08	12.183
Physical mixture of Formulation 09	21.655
Physical mixture of Formulation 11	23.657

Table 9: Parameters of the Model Equations Applied to the Release of Atorvastatin from Selected Nanocrystal Formulations

Formulation	Model	r <sup>2</sup>	Slope	K
F3	Zero order equation	0.9902	1.1603	0.9902
	First order equation	0.9188	0.0401	0.9585
	Higuchi model	0.9880	4.902	0.9902
	Peppas	0.8863	0.5891	1.1972
	Hixson-Crowell	0.9769	0.0567	2.047
F7	Zero order equation	0.9841	1.1885	0.9920
	First order equation	0.9480	0.0299	0.9737
	Higuchi model	0.9839	5.0019	0.9919
	Peppas	0.8848	0.4356	0.9839
	Hixson-Crowell	0.9658	0.0429	2.3753
F11	Zero order equation	0.9474	0.9733	1.139
	First order equation	0.8878	0.9422	0.032
	Higuchi model	0.9307	0.9647	4.752
	Peppas	0.8867	1.0498	0.4752
	Hixson-Crowell	0.9513	2.2859	0.0452
F14	Zero order equation	0.9685	0.9641	1.499
	First order equation	0.9470	0.9731	0.0241
	Higuchi model	0.9454	0.9723	6.234
	Peppas	0.8721	0.7541	0.3649
	Hixson-Crowell	0.9741	2.7924	0.041

Table 10: Particle Size and EE of ATC Nanoparticles After 7 Days Storage at Room Temperature (RT) and 4°C

Formula	Storage conditions	d(0.5)(nm)	E.E(%)	P-Value*
F3	Fresh	114.6±2.0	74.4±2.87	
	RT	129.0±1.0	78.0±2.67	0.01
	4°C	125.3±2.8	86.4±3.26	0.008
F7	Fresh	108.6±6.3	80.0±1.45	
	RT	152.6±2.5	87.5±2.33	0.01
	4°C	121.6±1.5	84.5±1.56	0.01
F11	Fresh	117.0±1.7	70.5±2.45	
	RT	118.0±1.0	69.8±1.98	0.45
	4°C	119.6±0.5	68.1±2.96	0.13
F14	Fresh	109.0±1.0	67.8±2.03	
	RT	112.0±1.7	66.6±2.34	0.08
	4°C	113.0±2.6	68.2±2.55	0.13

Table 7: Invitro release profile of Formulations F1-F16 (F13-F16-Physical Mixture of Formulations F3, F8, F9 and F11)

Time (min)	%Drug release															
	F1	F2	F3	F4	F5	F6	F7	F8	F9	F10	F11	F12	F13	F14	F15	F16
10	3.1	4.5	10.8	7.9	5.6	8.2	7.8	2.5	4.23	6.4	5.2	1.0	5.6	7.8	5.64	4.32
20	17.5	23.75	31.25	21.25	15	18	10.1	5.50	7.43	8.3	9	3.88	12.5	15.1	9.27	9.8
30	26.42	30.23	37.81	32.7	21.4	23.7	25.5	14.58	13.4	11.6	13.1	6.5	28.1	23.8	17.1	11.99
40	30.30	38.21	45.23	39.1	26.3	28.2	30.12	16.8	15.23	16.3	14.23	8.2	33.2	29.6	21.2	14.52
50	35.43	41.78	59.43	45.5	29.1	32.93	37.3	28.72	19.63	20.9	15.2	10.9	36.4	34.3	24.7	17.13
60	43.28	49.7	68.77	52.0	36.9	40.31	46.5	59.30	32.82	35.3	26.6	15.8	48.7	47.0	31.8	21.02
70	51.21	57.65	73.2	59.1	46.0	47.97	55.45	69.13	44.36	41.0	35.2	30.6	57.7	53.3	42.3	34.83
80	57.95	62	81.4	68.3	52.7	55.43	61.38	72.95	52.16	51.3	42.01	38.5	65.6	62.7	50.2	46.72
90	62.3	68.23	83.4	69.23	58.7	61.27	65.89	73.92	59.61	59.61	44.25	41.8	71.2	71.2	59.8	51.28
100	64.75	70.1	86.3	70.8	60.7	66.53	71.87	75.98	61.92	61.8	46.4	47.8	76.5	76.3	66.2	56.93
110	71.22	74.34	91.0	75.25	68.3	77.69	85.31	86.02	75.41	74.4	52.9	60.2	82.1	82.6	79.1	61.5
120	76.65	78.27	95.65	84.7	70.0	88.91	90.97	91.14	82.41	80.78	61.5	64.9	92.3	89.3	85.8	66.25

## FIGURES

Figure 1:  $\lambda$  max of ATC in Phosphate buffer (pH6.8)

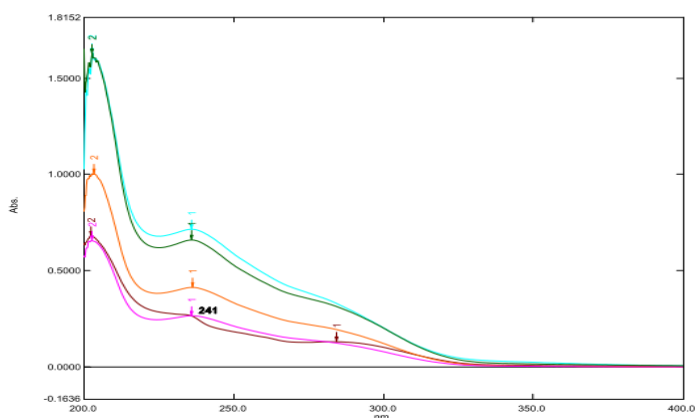


Figure 2: Calibration curve of ATC in Phosphate buffer (pH6.8)

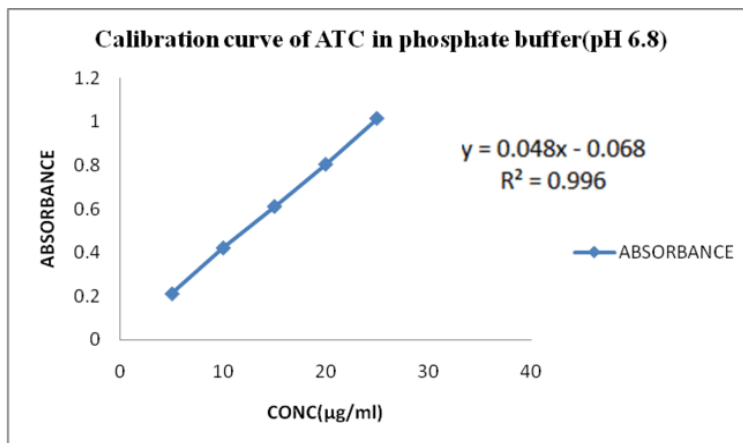
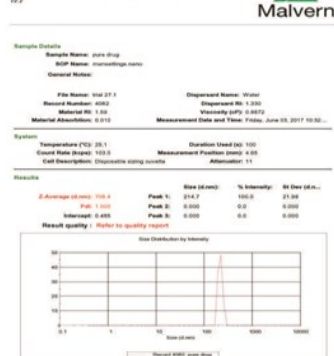


Figure 3: ZETA POTENTIAL

## Size Distribution Report by Intensity



## Size Distribution Report by Intensity



## Zeta Potential Report

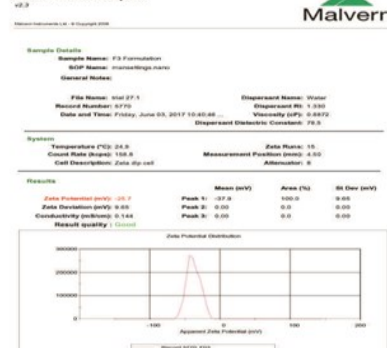


Figure 4: DISSOLUTION STUDIES

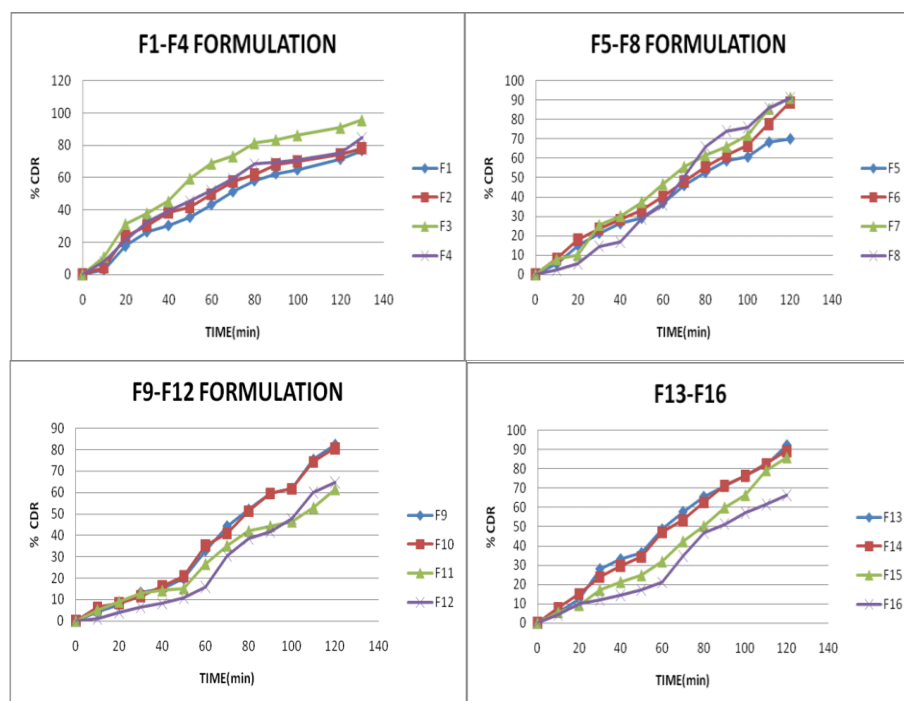


Figure 5: XRD OF PURE DRUG AND OPTIMIZED FORMULATION

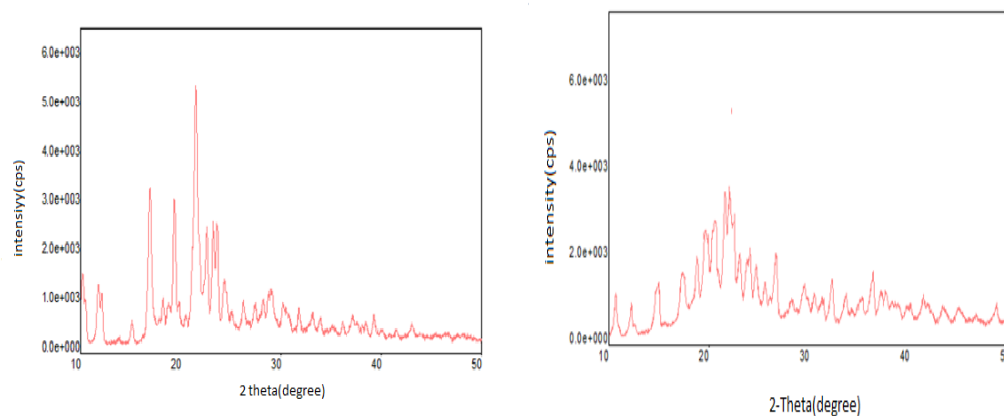


Figure 6: DSC THERMOGRAM OF PURE DRUG AND OPTIMIZED FORMULATION

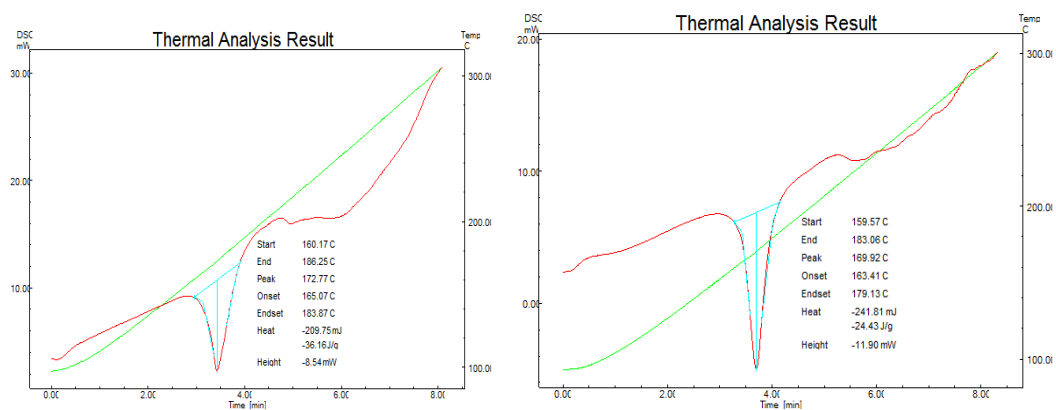


Figure 7: FTIR STUDIES OF PURE DRUG, PHYSICAL MIXTURE AND OPTIMIZED FORMULATION

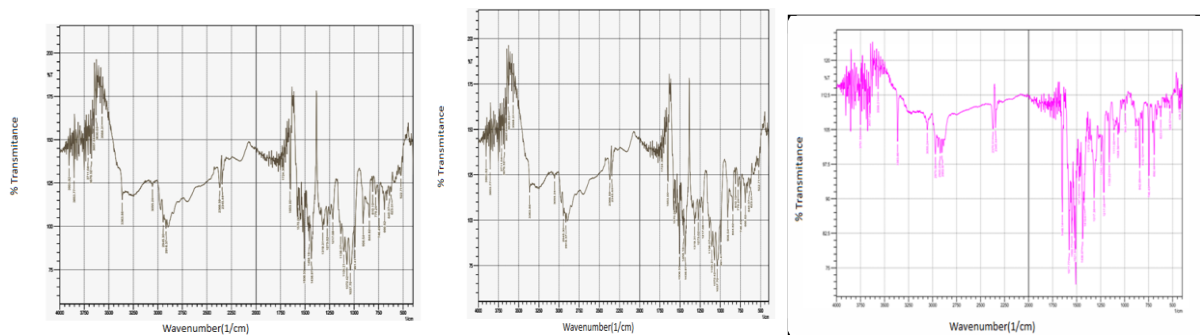


Figure 8: SEM IMAGES OF PURE DRUG AND OPTIMIZED FORMULATION

